2005-01-2813

Global Estimates of the Photosynthetically Active Radiation at the Mars Surface

J. M. Clawson and A. Hoehn
University of Colorado

ABSTRACT

This paper reports on the approach and progress to refine the estimates of the Mars surface photosynthetically active radiation (PAR) on a global scale that is averaged over a longer time period. While the PAR on Mars has been evaluated previously, the results have been limited in scope either temporally or spatially, such as only at a particular landing site or only over the time span of a few months. Understanding the availability of PAR is important in evaluating the practicality of using greenhouses and/or solar irradiance collectors for growing crops during manned missions to the Martian surface. Until surface investigations can be performed, computational modeling of the surface PAR can help to refine site selection and evaluation of engineering approaches and indicate the most favorable location at which to operate a greenhouse. The proposed approach is to combine multispectral irradiance models with global atmospheric opacity models developed from multiyear observations.

INTRODUCTION

This paper examines the availability of photosynthetically active radiation (PAR) at the surface of Mars. Photosynthetically Active Radiation (PAR) is that portion of the electromagnetic spectrum to which plants most respond and is generally between the wavelengths of 400-700nm (McCree 1972). While the PAR on Mars has been evaluated previously, the results have been limited in scope either temporally or spatially, such as only at a particular landing site or only over the time span of a few months (Ono and Cuello 2000; Ries, Bockstahler et al. 2003). This work proposes the combination of multispectral irradiance models with global atmospheric opacity models derived from multi-year orbital observations to arrive at an estimate of PAR across the planet surface throughout the year.

Understanding the availability of PAR is important in evaluating the practicality of using greenhouses and/or solar irradiance collectors for growing crops during manned missions to the Martian surface. Evaluating the practicality of using plants for life support is a major technical objective of The Advanced Life Support Technology Roadmap (Russo and Henninger 2002), an enabling question of NASA's Bioastronautics Critical Path Roadmap, and a top ten goal of the Mars Exploration Program Advisory Group (MEPAG) (Taylor, Sumner et al. 2004).

This paper does not presuppose a particular design implementation of a crop production system. Rather, the intention is to provide a model of an environmental variable which can then be used to arrive at a successful design. Furthermore, the efficacy of and analysis of threats to, e.g. radiation, micrometeorite, thermal control, a Mars greenhouse are covered elsewhere (see this conference Clawson, Hoehn et al. 2005).

EXISTING MARS PAR ESTIMATES - At an average orbital distance of 1.52 AU, Mars receives 43% of the solar input at the top of the atmosphere than that available at Earth's average orbital distance (1 AU). However, this varies from as little as 36% to as much as 52% that of Earth due to the orbital eccentricity of Mars. Figure 1 shows the spectrum at the top of the Earth's atmosphere compared to the spectra at the top of Mars' atmosphere during perihelion, aphelion, and at the average orbital distance each calculated using the inverse square law. The amount of light that reaches the surface, however, is more complicated involving absorption and scattering within the atmosphere.

On Earth, the amount of light that reaches the surface is a readily measured quantity. For example, the National Solar Radiation Database (NSRDB) contains 30 years (1961-1990) of solar radiation and supplementary meteorological data from 237 sites in the U.S., plus sites in Guam and Puerto Rico. Unfortunately, there is not an extensive measurement database of solar radiation on Mars. Only a handful of landers and rovers have taken surface irradiance data and only for limited time periods compared to a source such as the NSRDB.

Ono and Cuello (2000) used Viking 1 landing site calculated solar radiation data from Appelbaum, Landis et al. (1993) to estimate the PPF at the Mars surface. They determined a factor for converting the measured irradiance (Wm^{-2}) to PPF (4.568 $\mu mol m^{-2} s^{-1}/Wm^{-2}$ for Mars versus 4.609 $\mu mol m^{-2} s^{-1}/Wm^{-2}$ for Earth) given an estimated Mars surface spectrum from Crisp, Paige et al. (1994). They also estimated the percentage of PAR in the Mars surface spectrum to be 0.42. Their resulting estimated daily PPF averaged over the whole Martian year was 19.4 $molm^{-2}d^{-1}$.

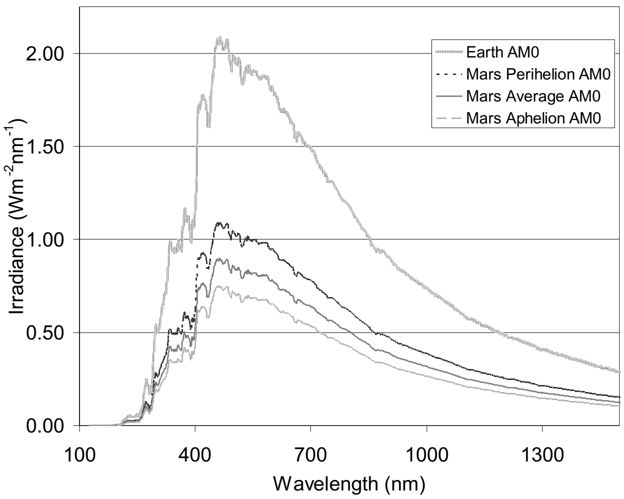

Figure 1 Top of atmosphere spectra at Earth and Mars including Mars at aphelion and perihelion. Data derived from ASTM-E-490-00a (2000).

Using the same conversion factors from Ono and Cuello, Figure 2 was generated to show the averaged daily PAR calculated from the average daily irradiance data from Appelbaum, Landis et al. The maximum was observed during the northern spring and summer when the PPF averaged ~25 $molm^{-2}d^{-1}$. Mars passes through perihelion during the northern autumn and winter and should have produced higher irradiances than observed, but there were two major planet-encircling dust storms during the measurement period making it one of the worst years observed (Appelbaum, Landis et al. 1993).

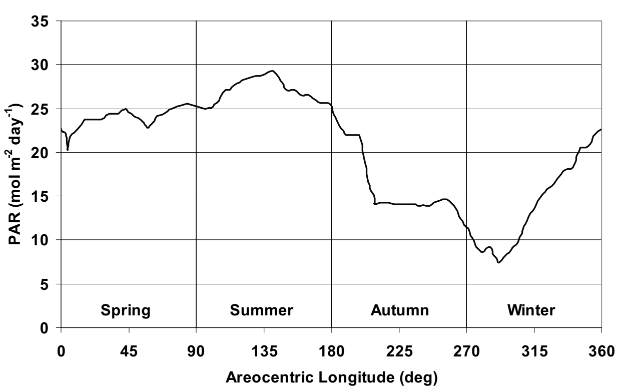

Figure 2 Averaged daily PAR incident on a horizontal plate at the Viking 1 landing site. Adapted from Appelbaum, Landis et al. (1993) using the relationships from Ono and Cuello (2000)

During the northern summer, the Viking 1 site received an average of 27 $molm^{-2}d^{-1}$, which is only 60% of that during a summer in Boulder, CO and is more comparable to what is received during an Alaskan summer. Alaska is known to support a small greenhouse growing industry, but how do these levels compare to those required for high performance plant growth targeted by NASA?

The required level of PAR for a crop depends on many factors including the plant type, age, environmental parameters, and desired crop performance. Table 1 lists the environmental parameters used for crop performance testing within the Biomass Production Chamber (BPC) at Kennedy Space Center and are good estimates of the light levels required for life support crops (Wheeler, Sager et al. 2003). The average daily PPF calculated by Ono and Cuello (2000) is enough to grow supplemental crops. For example lettuce, spinach, radish, beet, etc. were grown at a daily PPF of 17.28 mol/m^2 in the BPC (Wheeler, Sager et al. 2003).

Table 1 Environmental set points used for ALS candidate crops in KSC testing (Wheeler, Sager et al. 2003).

Crop (Genus species)	Photosynthetic Photon Flux (PPF) ($\mu mol\ m^{-2}\ s^{-1}$)		Photoperiod (hours)		Daily PPF ($mol\ day^{-1}$)
Staple Crops	Min	Max	Light	Dark	
Wheat (Triticum aestivum)	750	800	24	0	69.12
Soybean (Glycine max)	500	800	12	12	34.56
Potato (Solanum tuberosum)	500	800	12	12	34.56
Sweetpotato (Ipomoea batatas)	500	800	12	12	34.56
Peanut (Arachis hypogaea)	500	750	12	12	32.4
Rice (Oryza sativa)	750	800	12	12	34.56
Bean (Phaseolus vulgaris)	350	400	18	6	25.92
Supplemental Crops					
Lettuce (Lactuca sativa)	300		16	8	17.28
Spinach (Spinacia oleracea)	300		16	8	17.28
Tomato (Lycopersicon esculentum)	500	750	12	12	32.4
Chard (Beta vulgaris)	300		16	8	17.28
Radish (Raphanus sativus)	300		16	8	17.28
Red Beet (Beta vulgaris)	300		16	8	17.28
Strawberry (Fragaria x ananassa)	400	600	12	12	25.92

Depending on the efficiency of the light utilization (e.g. transparent structure, irradiance collectors, etc.), the available PPF at the Viking 1 landing site might be sufficient to grow some crops during part of the year. Even for higher light crops it is clear that the available natural insolation can go a long way in alleviating some of the high equivalent system mass (power mass, heat rejection mass, and physical mass) associated with artificial lighting. However, data from a single landing site over one Martian year is hardly enough to justify a full-scale greenhouse development program. Refining the estimate of Mars surface PAR on a global scale that is averaged over a longer time period will elucidate the utility and efficiency of direct solar crop lighting and could suggest the most favorable location at which to operate such a system.

SOLAR IRRADIANCE MODELING

With the lack of extensive measured data from the surface, estimating the surface PAR is left to modeling.

The solar irradiance at the surface of Mars is a function of

1. the variation in Mars-Sun distance due to the orbital eccentricity of Mars
2. the variation in solar zenith angle due to the Martian season and time of day
3. the opacity of the Martian atmosphere, primarily due to dust loading

The variation in the Mars-Sun distance and the solar zenith angle are readily calculated using orbital mechanics. However, the opacity of the Martian atmosphere is more complicated requiring detailed knowledge of the airborne aerosol characteristics, primarily dust. Once defined, the orbital and atmospheric opacity parameters can be used to solve the equation of radiative transfer.

Radiative transfer modeling has enabled the estimation of many phenomena related to Mars such as general circulation models (Pollack, Haberle et al. 1990), predicting the performance of solar power systems on the Martian surface (Appelbaum and Flood 1989; Haberle, McKay et al. 1993; Crisp, Pathare et al. 2003), and assessing the effects of the Martian UV on the survival of biological systems (Cockell, Catling et al. 2000; Schuerger, Mancinelli et al. 2003; Patel, Berces et al. 2004). Various methods have been employed to solve the equation of radiation transfer such as the delta-Eddington approximation (Joseph, Wiscombe et al. 1976; Patel, Zarnecki et al. 2002), the doubling/adding numerical method (Pollack, Toon et al. 1976; Pollack, Haberle et al. 1990), and discrete-ordinate numerical method (Stamnes, Tsay et al. 1988; Crisp, Pathare et al. 2003). Besides the solver employed, models are distinguished from one other by the number of environmental factors that are taken into account such as albedo, absorption and scattering from atmospheric gases, water vapor, and dust. Finally, as the fidelity of atmospheric property data increases, the surface irradiance can be computed at individual wavelengths. A multispectral code captures the effects of spectrally varying properties and is desired in this case to allow extraction of the PAR wavelengths.

The selected approach is to use output results from the code described by Crisp, Pathare et al. (2003). This code solves the monochromatic equation of transfer in plane-parallel, vertically inhomogeneous, scattering, absorbing, emitting atmospheres. A multi-level, multi-stream discrete ordinate algorithm, DISORT, was employed (Stamnes, Tsay et al. 1988). The wavelength dependence of the atmospheric and surface optical properties and source functions was accounted for by incorporating DISORT into the spectral mapping atmospheric radiative transfer (SMART) model. The SMART model interpolates wavelength-dependent atmospheric and surface optical properties and the solar source function onto a common spectral grid that resolves all of the spectral features of the input fields. It then evaluates the solar radiation field at each wavelength using high-resolution spectral mapping methods. Running the radiative transfer code for each time point in the day for each location on the surface at each position in the orbit is impractical. However, the analysis performed by Crisp, Pathare et al. (2003) involved solution of the model for a range of solar zenith angles at various dust levels. The zenith angle data can be mapped to the time of day depending on the latitude and orbit position while the discrete dust levels could be interpolated to account for latitudinal or even longitudinal variation in atmospheric conditions.

The multispectral nature of the Crisp model permits easy extraction of the PAR component. Once the irradiance data for the PAR wavelengths were isolated, the irradiance at each wavelength interval was quantized according to:

$$E = \frac{hc}{\lambda}$$

The spectrum of PPF fluxes was then integrated. Figure 3 shows the resulting integrated PPF versus solar zenith angle [θ_0 = 0°, 20°, 35°, 50°, 65°, 75°, 85°, 90°] at 9 different dust optical depths [τ_d = 0.001, 0.1, 0.3, 0.6, 1.0, 2.0, 3.0, 4.0, 5.0].

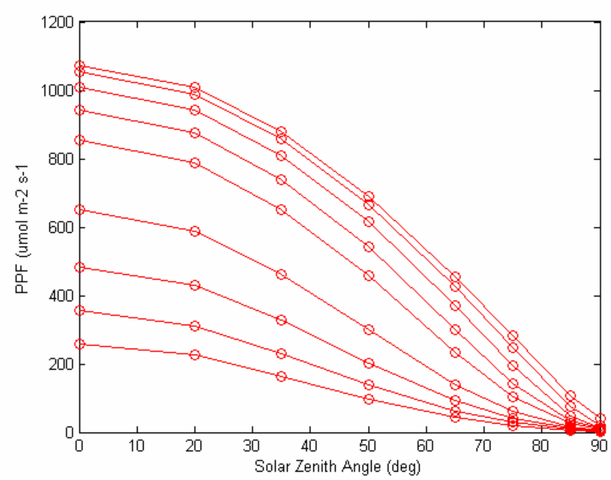

Figure 3 The PPF versus solar zenith angle for 9 different dust optical depths (from top to bottom: τ_d = 0.001, 0.1, 0.3, 0.6, 1.0, 2.0, 3.0, 4.0, 5.0) at a Mars orbital distance of 1.5 AU.

Crisp, Pathare et al. (2003) included irradiance calculations at four different dust levels (0.1, 0.5, 1.0, and 5.0). Even though these levels cover the expected range of dust optical depths likely to be encountered, four levels are not enough to accurately interpolate the irradiance at intermediate depths. Figure 4 shows the PPF versus optical depth for each of the solar zenith angles. The figure shows that the increased number of optical depths will ensure accurate interpolation.

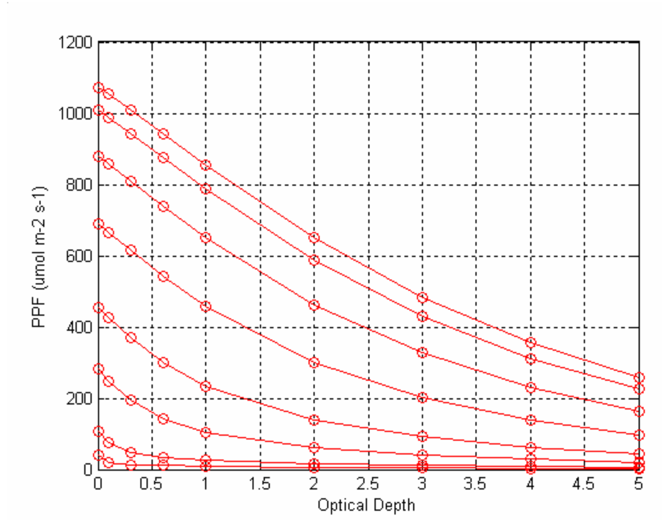

Figure 4 Photosynthetic Photon Flux (PPF) vs. dust optical depth at 8 different solar zenith angles at Mars orbital distance of 1.5 AU.

The modeled photosynthetic flux data can be further be normalized to the flux available at the top of the atmosphere. This allows the use of the data throughout the change solar distance experience by Mars during its orbit. The additional model runs have produced enough data to allow accurate interpolation within the expected range of dust levels. The next step is to marry the modeled photosynthetic flux data with global aerosol data.

MARS DUST MODELS

We have just begun the search for an appropriate dust distribution with which to combine our PPF model. Fortunately, there are a growing number of planet-wide databases of Mars atmosphere characteristics thanks to recent Mars exploration spacecraft.

Lewis, Collins et al. (1999) have developed a dust distribution based on data from the Mars Global Surveyor. Figure 5 shows the dust levels as a function of season (areocentric longitude, Ls) and latitude. While this model offers good temporal resolution, the lack of spatial resolution does not allow the comparison of the available PPF at various locations across the planet's surface. In contrast, Figure 6 shows the dust optical depth measured by the Mars Odyssey THEMIS. The top graph shows the seasonal variation (Ls, areocentric longitude or orbit position) versus latitude while the bottom graph shows the variation over the planets surface over a time span encompassing 20° of areocentric longitude (Smith, Bandfield et al. 2003). It is obvious that there is a trade-off between spatial and temporal resolution.

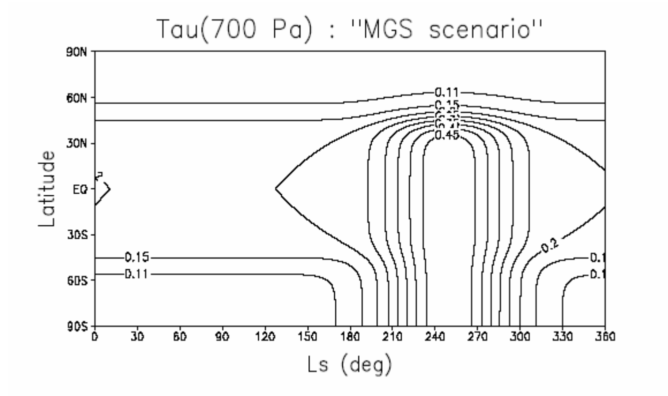

Figure 5 Variation of the reference optical depth at 700 Pa as a function of season (solar longitude L_s) and latitude in the MGS scenario.(Lewis, Collins et al. 2001)

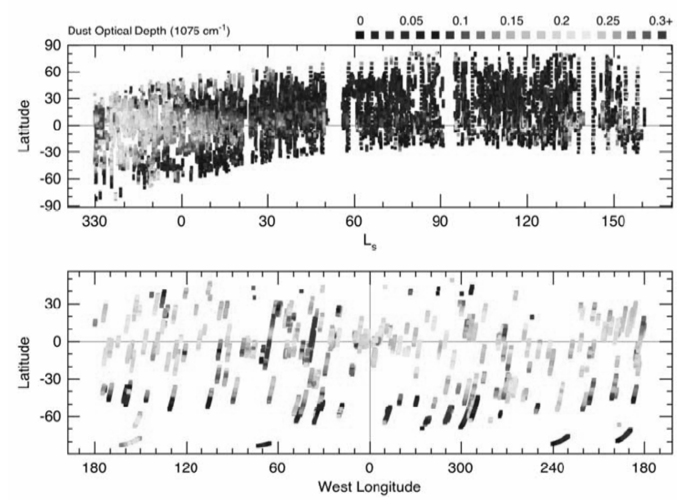

Figure 6 Dust optical depth measurements from the Mars Odyssey THEMIS. (Top) Seasonal variation of dust aerosol versus latitude. (Bottom) Spatial (latitude vs. longitude) measurements of dust optical depth taken over 20° of areocentric longitude (Smith, Bandfield et al. 2003).

The distribution developed by Lewis, Collins et al. will be used initially to validate the interpolation and integration protocols. In the meantime, we will search for a distribution with the best combination of the temporal and spatial resolution.

CONCLUSION

In this paper we have outlined an approach to refining the estimates of the Mars surface PAR on a global scale. The proposed approach combines the results of high spectral resolution irradiance models with globally varying dust distribution scenarios. The increased spectral resolution of the modeled irradiance improves the accuracy of the extraction of photosynthetic photon flux data. However, there are some limitations to this approach. The only parameters that are varied in the resulting dataset are zenith angle and dust optical depth. The affect of local variation in albedo, altitude, and atmospheric pressure are ignored. However, the variation in the normalized net flux function used in Appelbaum, Landis et al. (1993) varies less than 5% between and albedo of 0.1 and 0.4 at the same dust optical depth of 1.0. More analysis is needed to quantify the possible error due to variation in altitude and atmospheric pressure. Additionally, although the effect of atmospheric water vapor is explicitly accounted for in the model, atmospheric water column abundance varies spatially and temporally, which has not be taken into account. Finally, the dust absorption and scattering characteristics change with the type of material from which the dust originated. The dust characteristics vary over the planet's surface and will not be taken into account. All of the sources of variation will be addressed and evaluated in the final analysis.

ACKNOWLEDGMENTS

This work was supported by NASA through the Graduate Student Research Program (NGT10-52624) and BioServe Space Technologies - Research Partnership Center under a Cooperative Agreement (NCC8-242). The authors would also like to thank Dr. David Crisp for radiative transfer modeling.

REFERENCES

1. Appelbaum, J. and D. J. Flood (1989). Photovoltaic Power System Operation in the Mars Environment. 102075, Cleveland, OH, NASA Lewis Research Center.
2. Appelbaum, J., G. A. Landis, et al. (1993). "Solar-Radiation on Mars - Update 1991." Solar Energy 50(1): 35-51.
3. ASTM-E-490-00a (2000). Standard: Solar Constant and Zero Air Mass Solar Spectral Irradiance Tables. West Conshohocken, PA, ASTM: 16.
4. Clawson, J. M., A. Hoehn, et al. (2005). Inflatable Transparent Structures for Mars Greenhouse Applications. 35th International Conference on Environmental Systems, Rome, Italy, SAE.
5. Cockell, C. S., D. C. Catling, et al. (2000). "The Ultraviolet Environment of Mars: Biological Implications Past, Present, and Future." Icarus 146: 343-359.
6. Crisp, D., D. A. Paige, et al. (1994). The performance of solar cells at the Martian surface. Pasadena, CA, Jet Propulsion Laboratory.
7. Crisp, D., A. Pathare, et al. (2003). "The performance of gallium arsenide/germanium solar cells at the Martian surface." Acta Astronautica 54(2): 83-101.
8. Haberle, R. M., C. P. McKay, et al. (1993). Atmospheric Effects on the Utility of Solar Power on Mars. Resources of Near-Earth Space. J. Lewis, M. S. Matthews and M. L. Guerrieri. Tuscon & London, The University of Arizona Press: 845-885.
9. Joseph, J. H., W. J. Wiscombe, et al. (1976). "The delta-Eddington approximation for radiative flux transfer." Journal of the Atmospheric Sciences 33(12): 2452-2459.
10. Lewis, S. R., M. Collins, et al. (2001). Mars Climate Database V3.0 Detailed Design Document.
11. Lewis, S. R., M. Collins, et al. (1999). "A climate database for Mars." Journal of Geophysical Research-Planets 104(E10): 24177-24194.
12. McCree, K. M. (1972). "The Action Spectrum, Absorbance and Quantum Yield of Photosynthesis in Crop Plants." Agricultural Meteorology 9: 191 - 216.
13. Ono, E. and J. Cuello (2000). Photosynthetically Active Radiation on Mars. 30th International Conference on Environmental Systems, Toulouse, France, Society of Automotive Engineers.
14. Patel, M. R., A. Berces, et al. (2004). "Annual solar UV exposure and biological effective dose rates on the Martian surface." Advances in Space Research 33(8): 1247-1252.
15. Patel, M. R., J. C. Zarnecki, et al. (2002). "Ultraviolet radiation on the surface of Mars and the Beagle 2 UV sensor." Planetary and Space Science 50(9): 915-927.
16. Pollack, J. B., R. M. Haberle, et al. (1990). "Simulations of the general circulation of the Martian atmosphere: I. Polar processes." Journal of Geophysical Research 95: 1447-1473.
17. Pollack, J. B., O. B. Toon, et al. (1976). "Estimates of Climatic Impact of Aerosols Produced by Space Shuttles, SSTs, and Other High Flying Aircraft." Journal of Applied Meteorology 15(3): 247-258.
18. Ries, R., S. Bockstahler, et al. (2003). RedThumb: A Mars Greenhouse Design for the 2002 MarsPort Engineering Design Student Competition. 33rd International Conference on Environmental Systems, Vancouver, BC, SAE.
19. Russo, D. M. and D. L. Henninger (2002). Advanced Life Support Project Plan. CTSD-ADV-348 Rev C, JSC 39168, Houston, TX, Crew and Thermal Systems Division, Lyndon B. Johnson Space Center, National Aeronautics and Space Administration.
20. Schuerger, A. C., R. L. Mancinelli, et al. (2003). "Survival of endospores of Bacillus subtilis on spacecraft surfaces under simulated Martian environments: Implications for the forward contamination of Mars." Icarus 165: 253-276.
21. Smith, M. D., J. L. Bandfield, et al. (2003). "Thermal Emission Imaging System (THEMIS) infrared observations of atmospheric dust and water ice cloud optical depth." Journal of Geophysical Research-Planets 108(E11).
22. Stamnes, K., S. C. Tsay, et al. (1988). "Numerically Stable Algorithm for Discrete-Ordinate-Method Radiative-Transfer in Multiple-Scattering and

Emitting Layered Media." Applied Optics 27(12): 2502-2509.
23. Taylor, G. J., D. Sumner, et al. (2004). Scientific Goals, Objectives, Investigations, and Priorities: 2004. Reference# CL#04-0387 (http://mepag.jpl.nasa.gov/reports/index.html), Pasadena, CA, Jet Propulsion Laboratory MEPAG (Mars Exploration Program Analysis Group).
24. Wheeler, R. M., J. C. Sager, et al. (2003). Crop Production for Advanced Life Support Systems - Observations From the Kennedy Space Center Breadboard Project. NASA/TM-2003-211184, Kennedy Space Center, Florida, National Aeronautics and Space Administration.

CONTACT

Jim Clawson is a PhD candidate in the Aerospace Engineering Sciences department at the University of Colorado in Boulder. He can be reached at:

University of Colorado
Engineering Center ECAE 152
Boulder, CO 80309
(303) 492-2341

DEFINITIONS, ACRONYMS, ABBREVIATIONS

DISORT: Discrete-Ordinate Radiative Transfer

NSRDB: National Solar Radiation Database

PAR: Photosynthetically Active Radiation

PPF: Photosynthetic Photon Flux

SMART: Spectral Mapping Atmospheric Radiative Transfer Model

THEMIS: Thermal Emission Imaging System